INTEGRATED SEISMIC EVENT DETECTION AND LOCATION BY ADVANCED ARRAY PROCESSING

T. Kvaerna[1], S. J. Gibbons[1], F. Ringdal[1], and D. B. Harris[2]

NORSAR[1] and Lawrence Livermore National Laboratory[2]

Sponsored by National Nuclear Security Administration
Office of Nonproliferation Research and Development
Office of Defense Nuclear Nonproliferation

Contract Nos. DE-FC52-03NA99517[1] and W-7405-ENG-48[2]

ABSTRACT

As the trend in nuclear explosion monitoring continues in the direction of detecting and locating seismic events of ever smaller magnitudes, the number of events which are detected and which require processing increases enormously. With more candidate phase determinations and event hypotheses, it is of paramount importance that the accuracy of parameter estimates and automatic event locations is good enough to prevent analyst time being used on examining signals which can, with a high level of confidence, be attributed to known industrial seismic sources. It is similarly important to try to maintain a low false alarm rate. Many seismic arrays of the International Monitoring System (IMS) are within regional distances of many sources of repeating seismic events. In recently funded studies, large numbers of events from known sources of seismicity have been identified providing an excellent basis of ground-truth (GT) events by which we have been able to benchmark phase determinations and subsequent event location estimates. Some of these events are mining events for which the mine operators have provided explosion times and locations, and other events have been attributed to source locations on the basis of waveform correlation studies.

The aim of the current project has been to construct a prototype system for the automatic monitoring of seismic events from sites of interest using regional seismic arrays. Current automatic location procedures frequently show rather large mislocations. In many cases, this is due to multiple events whereby several sequences of similar regional phases may reach a given seismic array within a short time period and be subsequently associated incorrectly. The prototype system is designed to mitigate errors of this kind by considering a system of *site-templates* whereby, under the hypothesis of an event at a given time from a calibrated source location, we consider only the observation of wavefield parameters in a number of very carefully defined time-windows relative to the hypothetical origin time. Another major source of error in the current automatic location estimates is a result of the use of azimuth and slowness estimates measured using variable frequency bands which show a demonstrably greater spread than the corresponding estimates measured in fixed frequency bands. The prototype system is designed to mitigate these errors by using a calibrated *phase-template* for each of the time-windows specified by the site-template. Azimuth and slowness are measured in one or more fixed frequency bands which are demonstrated to give the most stable estimates for a given phase from a given site, and appropriate corrections are applied prior to the location procedure. The template-based system gives automatic location estimates which are demonstrably better for the sites considered than the corresponding generalized beamforming (GBF) solutions. Anticipated and observed azimuth values can vary dramatically, emphasizing the need for calibration.

An additional problem with site- or phase-templates relying upon conventional frequency wavenumber (F-K) analysis and beamforming is the loss of coherence across an array aperture. Conventional algorithms assume that the wavefields incident upon an array satisfy a plane-wave model. When they do not, as happens when refraction and scattering are significant, especially in higher frequency bands, empirical matched-field processing may improve performance. In the matched-field processing approach, narrowband plane-wave steering vectors are replaced with empirical steering vectors derived from many observations of the array signal of interest. Last year we demonstrated empirical steering vectors for the ARCES array for the Pn phase from mines of the Khibiny Massif. These calibrations provided up to a factor of 3 improvement in energy detection at frequencies above 10 Hz. This year we report progress on extending the calibration from a single phase to the entire seismogram. The innovation is a non-stationary calibration or set of steering vectors that changes continuously throughout the duration of the seismogram as different phases come and go.

OBJECTIVE

This two year collaboration between the Norwegian Seismic Array (NORSAR) and Lawrence Livermore National Laboratory (LLNL) has explored improvements to the automatic detection and location of seismic events using regional arrays. At the heart of the study has been the calibration of processing parameters for the detection and location of events from a specific region using observations of previous ground-truth events at the sites of interest. The goal is to attribute, with a high degree of confidence, automatically located events to active mines or areas with known recurring seismicity. The study has examined sites in Fennoscandia and Kazakhstan using the seismic arrays in these regions.

The signals at a given array station, resulting from a set of events from a site with recurring seismicity, are likely to display common characteristics which may be exploited in order to identify subsequent events from the same region. A template describing the measurements which can be anticipated at a given station at a given time can be used to judge whether or not a detected signal is the likely result of an event from the site of interest. Such templates must be calibrated by investigating the variability of measurements made from events confirmed to have taken place at the sites; such calibrations have been the main focus of this investigation. We have, in addition, explored the potential of applying advanced new "matched field" array processing methods in order to compensate for array processing loss due to refraction and scattering, thus enhancing array gain at high frequencies.

RESEARCH ACCOMPLISHED

Automatic Event Detection and Location Procedures

The aims of nuclear explosion monitoring are being widened continually to encompass the detection, location, and identification of seismic events of ever smaller magnitude. This leads to a dramatic increase in the number of seismic events which require processing which in turn leads to increased demands upon automatic processing procedures. Such procedures need to be sensitive (to ensure that no events are missed), with a low false-alarm rate, and accurate. In particular, the large number of routine industrial seismic events should be associated (fully-automatically and with a high level of confidence) with the correct source location. Recent improvements in GT information for repeating seismic sources have improved dramatically our ability to assess the quality of fully automatic event location estimates. Figure 1 shows the location of numerous sites of repeating seismicity in northern Fennoscandia and north-west Russia for which we have excellent GT information. The four regions indicated in Russia are all sites of several different mines and information regarding the location and origin times of explosions has been collected from all these sites under the NNSA-funded contract "Ground-truth Collection for Mining Explosions in Northern Fennoscandia and Russia" (Harris et al., 2003). Explosions at the Finnish ammunition destruction site were identified largely from the GBF (Kvaerna and Ringdal, 1989) automatic event bulletin due to the characteristic explosion times; their identification was subsequently confirmed using array-based waveform correlation (Gibbons and Ringdal, 2006) which also provided excellent constraints upon the origin time of each event. For the remaining sites (all large-scale mining operations in the north of Sweden), information regarding a few selected events was provided by the mining companies, and large numbers of additional events were subsequently identified using waveform correlation methods. Figure 1 (a,b) allows a direct comparison of known event locations and fully-automatic GBF location estimates. Whilst the location accuracy is generally sufficiently good for an analyst to take an event and relocate it interactively, it is clear that associating signals with a specific source region is not possible without some form of post-processing algorithm. The reasons for the large spread in the GBF solutions are well-understood and motivate the development of a template-based system as depicted in Figure 2. Observations of many events from the same source region allow for a very good evaluation of which phases are well-observed at which stations and at which times following a seismic event; this is the concept of a site template. Within a carefully defined time-window for each such phase, we can define a set of diagnostic tests together with a range of accepted values by which we can determine whether or not the observed phase is consistent with corresponding observations from previous events at the same site. This is the concept of a phase template (see Figure 3). Gibbons et al. (2005) describe in detail the algorithm and results for such a system for the identification and location of events from the Kovdor mine. In this case, observations from only a single array station are used. This is a case of increasing relevance in the observation of increasingly small events using a relatively sparse international seismic network.

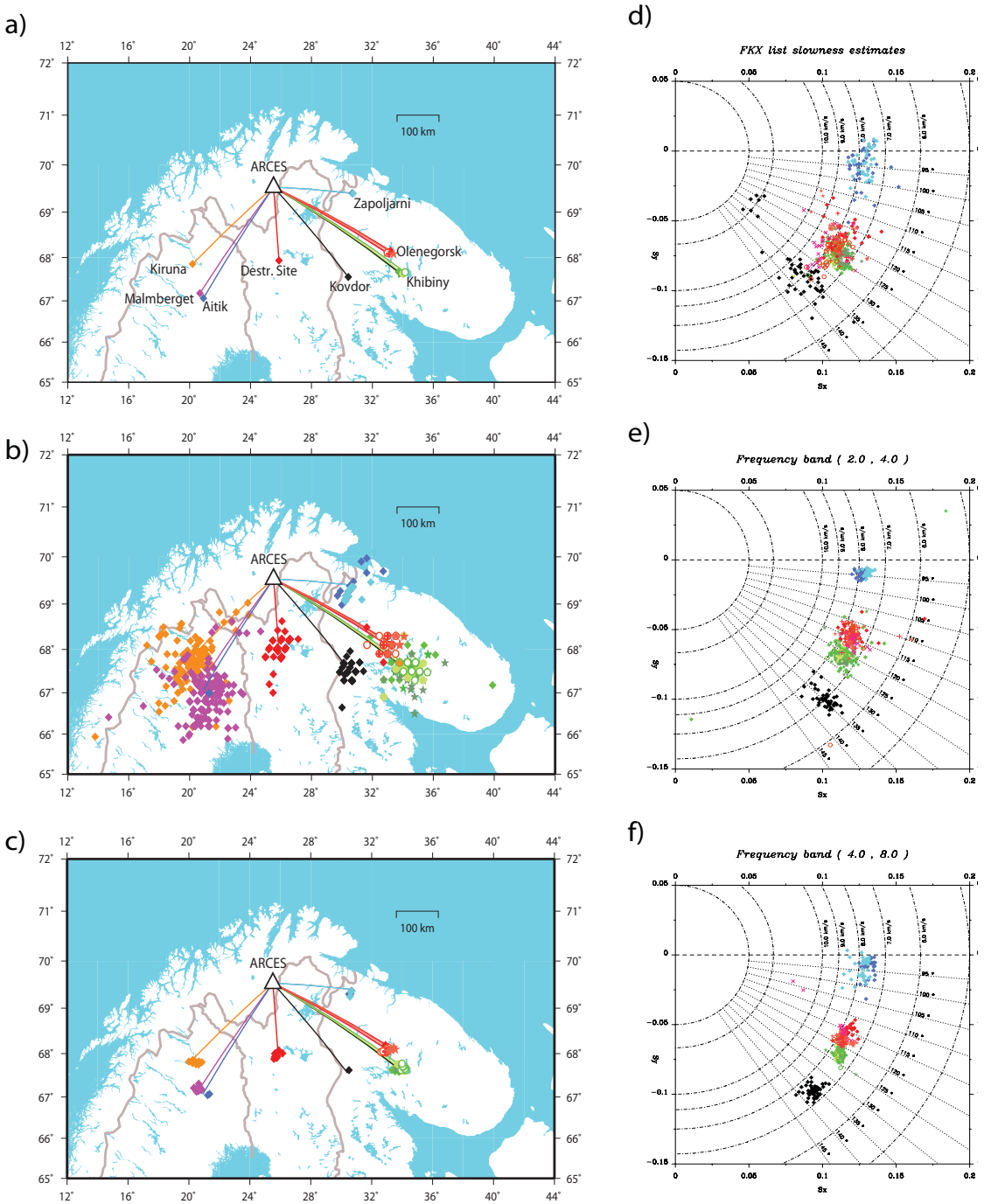

Figure 1. (**a) Sites of repeating seismicity in the vicinity of the ARCES primary IMS array. (b) Fully automatic location estimates (Kværna and Ringdal, 1989) for events known to have taken place at the sites in (a). (c) Analyst reviewed location estimates for selected events from (b). (d) fully automatic slowness vector estimates for initial P-arrivals for events from the mining sites on the Kola Peninsula in North West Russia (Zapoljarni, Olenegorsk, Khibiny, Kovdor). (e) Fixed frequency band slowness estimates (2.0 - 4.0 Hz) for the arrivals displayed in (d). (f) the same phase arrivals processed in the fixed frequency band 4.0 - 8.0 Hz.**

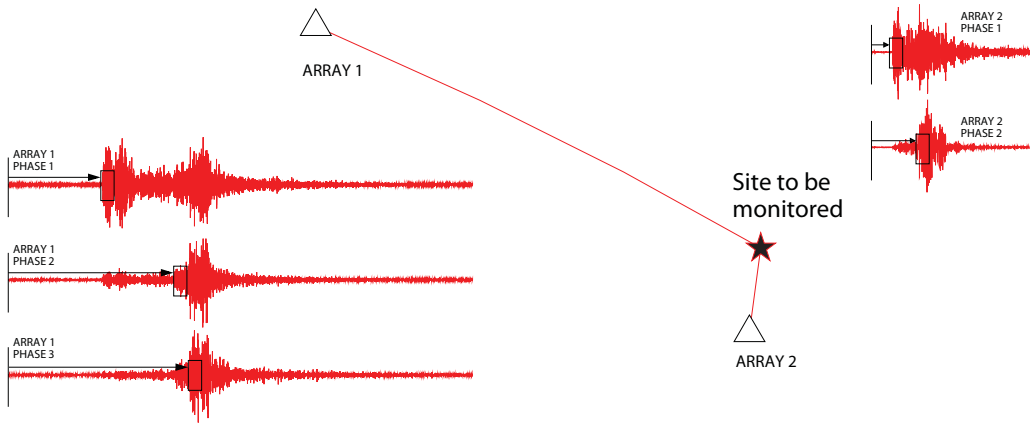

Figure 2. Schematic representation of a template-based event identification and location algorithm. The site template specifies which seismic phases should be observed at which times at which stations, given a hypothesis of a seismic event at a site of interest at a given time. For each such phase, a phase-template (symbolized by the black boxes) defines a set of test parameters, evaluation criteria and, optionally, calibration information which determine whether or not the observed phase is consistent with observations of that phase from previous events at that site (see Figure 3).

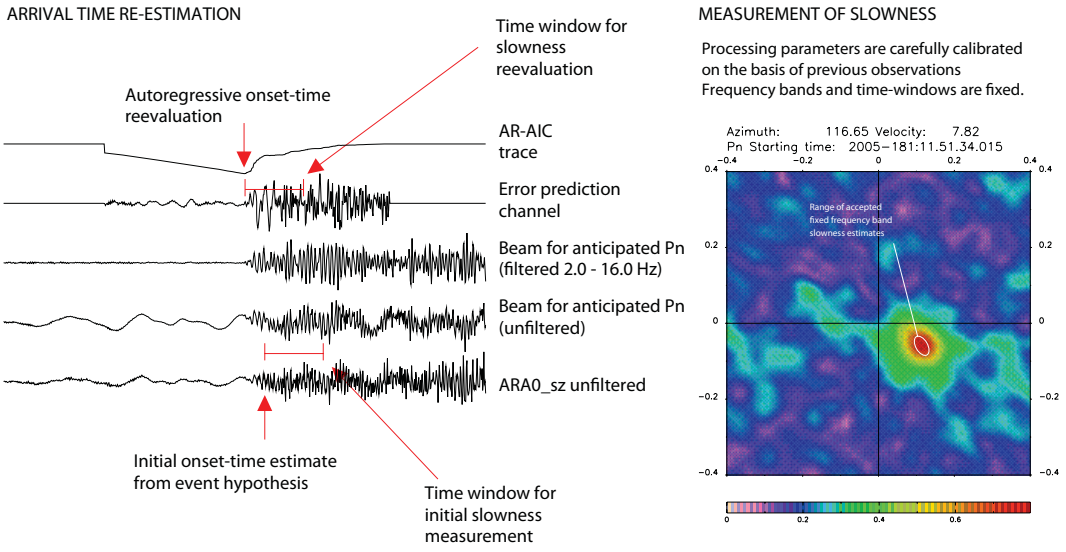

Figure 3. The principal components of a site template in regional array event identification and location algorithms: autoregressive arrival time re-estimation (left) and measurement of backazimuth and apparent velocity using broadband F-K analysis in fixed frequency bands. As displayed in Figure 1 (d,e,f), the use of carefully chosen fixed frequency bands can lead to a great improvement in the stability of slowness estimates and allows for far tighter hypothesis acceptance criteria.

Under the current project (Kværna et al. 2004, 2005), the principles applied in Gibbons et al. (2005) have been extended to encompass a far wider range of sites and station configurations. In all cases, the application of template-based algorithms has led to an improvement in fully-automatic event location estimates. In almost all cases in which the procedure failed, the reason for failure was the rejection of event hypotheses due to the inability to measure a phase arrival time with a sufficient level of confidence (signal-to-noise ratio [SNR] or Akaike Information

Criterion measurements did not satisfy required thresholds) or the failure of F-K analysis to return a slowness estimate within the required time-window. In almost all cases, this was the result of "interfering signals" which were almost invariably multiple events from the same site. Such multiple event sequences are unfortunately very characteristic of the type of event we are attempting to classify in the current investigation. In the GBF algorithm, this typically leads to a spurious association of P- and S- phases from distinct events and a corresponding location estimate at the wrong site (see Figure 1b). This eventuality is precluded from the template-based system since we only consider observations within the time-windows defined by the site-template (Figure 2); phases observed outside of these time intervals have no influence on the evaluation of the event hypothesis. Gibbons et al. (2005) found that approximately 40% of the confirmed Kovdor events could not be located automatically due to such interfering phases. To deal with this eventuality, a new category "very likely Kovdor events" was defined; these are signals which show many characteristics of events from the site of interest, albeit not sufficiently many that the event can be located automatically. This category is useful but a setback in our quest to mitigate the need for analyst interaction. It is useful to note that in the cases where a fully automatic location was not possible, the analyst location was also subject to a far higher degree of error. This failure rate (40% of events not locatable) turned out to be quite typical for all the sites covered.

Considerations in the Use of Small-Aperture Arrays for Slowness Measurements and Consequences for Event Location Etimates

Whilst the majority of the location estimates in Figure 1b which are "qualitatively incorrect" are the result of spurious phase association, the general large spread in location estimates is primarily the result of applying slowness and azimuth estimates which are measured in variable frequency bands. Figure 1d shows slowness estimates for the initial P-arrivals from the Russian events in the dataset, measured in a frequency band optimized on an event-by-event basis, as they appear in the NORSAR detection lists. Figure 1 e) and f) show the slowness estimates for exactly same arrivals when measured in the fixed frequency bands 2.0-4.0 Hz and 4.0-8.0 Hz respectively. Two results are immediately evident:

1. The fixed frequency band estimates are far more stable than the variable band estimates.
2. The frequency band offering the most stable estimate is not the same for all sites.

It is, for example, clear how the spread in slowness estimates for the Zapoljarni mines (blue symbols) in Figure 1d translates directly into the spread in event location estimates observed in Figure 1b. It is likely that if only slowness estimates obtained in the 2.0 - 4.0 Hz band were applied, then the corresponding spread in location estimates would decrease dramatically. If the slowness estimates obtained between 4.0 and 8.0 Hz were used instead, the spread in location estimates would probably remain large. The situation is reversed for the Khibiny mines with the higher frequencies resulting in more stable estimates.

The set of Finnish explosions provides a nice example case since, due to the simpler source-time functions, none of the events were subject to interfering phases and the spread in event location estimates can be attributed almost entirely to variable slowness estimates and error in phase onset-time measurements. Figure 4 shows the fully-automatic P-phase slowness estimates (left) and the same estimates made in the fixed frequency bands as indicated (right). The fixed-band estimates not only display a significantly lower spread for each band applied, but also display almost no overlap between the different bands. It is important to note that at this epicentral distance, a triplication occurs whereby the Pg crustal phase and the higher frequency Pn phase arrive essentially at the same time; this may explain why the velocity in the 4.0-8.0 Hz band is higher than the velocity at lower frequencies. At even higher frequencies, waveform incoherence over the array is probably significant. However, what is not explained by this triplication is how the azimuth varies with the frequency band. The smallest spread is observed for the 2-4 Hz band and restricting location estimates to these values results in location estimates for the fully-automatic template-based method which are superior to the analyst interactive location estimates (Figure 5). The reason for this is evident from Figure 4; the analyst picks a frequency band on an event-to-event basis and locates the event using velocity and azimuth measured in the chosen band. The analyst does not (currently) have the calibration information available and is not aware that the 2-4 Hz band gives by far the most stable azimuth estimates for events from this site. It must also be stressed that this result is by no means intuitive since the SNR is significantly lower in this frequency band than it is at higher frequencies. The temptation will be to use a frequency band which produces an optimal combination of SNR and high F-K power (beam gain) - this is judged subjectively by the analyst for each

event encountered and results consequently in a directional estimate which is a direct function of the frequency band applied.

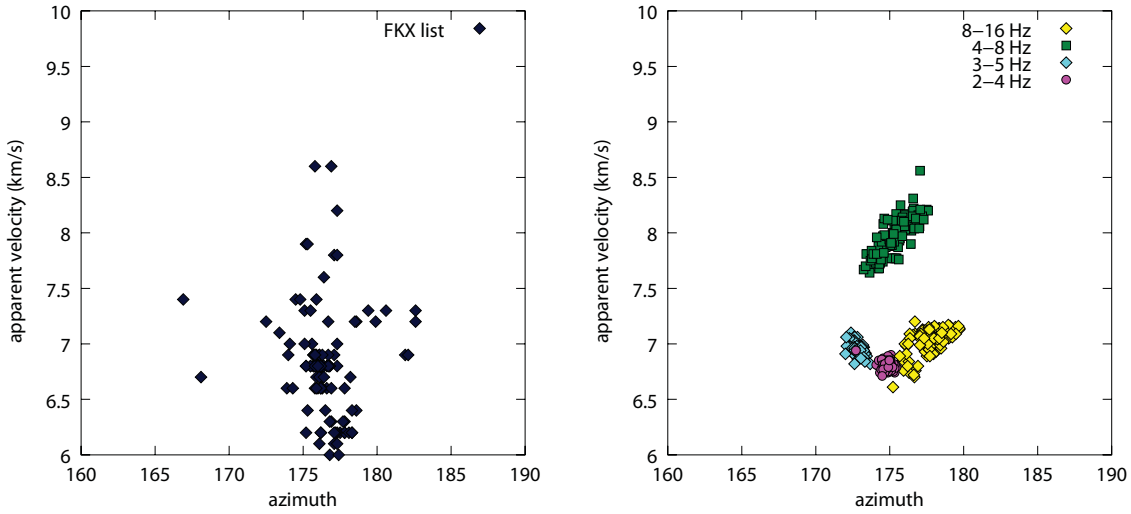

Figure 4. (Left) slowness estimates in the routine automatic processing for the defining P-arrival at the ARCES seismic array for each of 108 ammunition destruction explosions at a military site in the north of Finland, at a distance of approximately 175 km. (Right) slowness estimates for in the indicated fixed frequency bands for the same arrivals, albeit measured in an identical time window for each event.

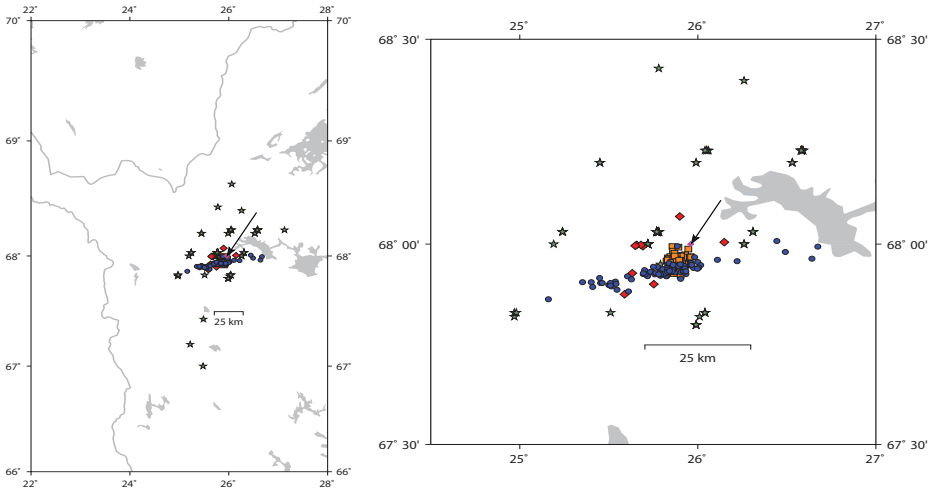

Figure 5. Locations of Finnish explosions using different location methods. The exact explosion site coordinates are not known but are assumed to be approximately 68°N, 26°E (see arrow), the green stars represent the GBF fully-automatic location estimates, the red diamonds indicate the NORSAR analyst reviewed location estimates, the orange squares indicate the single array (ARCES) template-based location estimates, and the blue circles indicate the 3-component station network solutions using the Finnish National Seismic Network (courtesy of the seismic bulletin of the University of Helsinki). Note in particular how the template-based fully automatic solutions have a far lower standard error (approximately 5 km) than either the NORSAR reviewed analyst solutions (approximately 15 km) or the Finnish network solutions.

Matched Field Processing

Last year, we tested the concept of applying empirical matched field processing to a single phase (Pn) at high frequencies (above 10 Hertz) for a small aperture array (ARCES). For a single phase it is reasonable to make the assumption that the spatial statistics of the signal are stationary. Using a narrowband (essentially monochromatic) assumption, we made the approximation that the complex analytic form of the array signal in a narrow band centered on frequency $\mathbf{f}_0$ has the form:

$$\underline{\mathbf{r}}(\mathbf{t}) = \begin{bmatrix} \mathbf{r}(\underline{\mathbf{x}}_1, \mathbf{t}) \\ \mathbf{r}(\underline{\mathbf{x}}_2, \mathbf{t}) \\ \\ \mathbf{r}(\underline{\mathbf{x}}_N, \mathbf{t}) \end{bmatrix} = \underline{\varepsilon}(\mathbf{f}_0)\mathbf{s}(\mathbf{t}, \mathbf{f}_0)\mathbf{e}^{-\mathbf{i}2\pi\mathbf{f}_0\mathbf{t}} \qquad (1)$$

where the signals $\mathbf{r}(\underline{\mathbf{x}}_\mathbf{i}, \mathbf{t})$ are the signals recorded by individual sensors in the array located at positions $\underline{\mathbf{x}}_\mathbf{i}$. The baseband signal $\mathbf{s}(\mathbf{t}, \mathbf{f}_0)$ is a slowly-varying complex envelope. This narrowband approximation has the effect of separating the spatial and temporal variations of the signal into multiplicative factors. The so-called steering vector $\underline{\varepsilon}(\mathbf{f}_0)$ encodes all of the spatial variation of the signals across the array, and the baseband signal encodes the remaining temporal structure. This approximation becomes more accurate the narrower the processing band and becomes exact for monochromatic signals.

In the plane-wave approximation, the steering vector embodies the complex phase factors induced by propagation delays across the array. In a reality, effects of refraction (e.g. focusing), diffraction, and scattering cause the steering vector to depart from this simple model. As a consequence, we advocate measuring the steering vector for particular source regions as a calibration and applying the measured steering vector in FK and beamforming operations instead of its theoretical plane-wave counterpart. Measuring the steering vector is conceptually straightforward using a large number (*M*) of waveforms from events in the target region of interest. We recommend estimating the spatial covariance matrix over the ensemble of events as:

$$\underline{\mathbf{R}}(\mathbf{f}_0) = \overline{\underline{\mathbf{r}}(\mathbf{t})(\underline{\mathbf{r}}(\mathbf{t}))^{\mathbf{H}}} \sim \frac{1}{\mathbf{M}} \sum_{\mathbf{j}=1}^{\mathbf{M}} \int \underline{\mathbf{r}}_\mathbf{j}(\mathbf{t})(\underline{\mathbf{r}}_\mathbf{j}(\mathbf{t}))^{\mathbf{H}} \mathbf{dt} = \alpha \underline{\varepsilon}(\mathbf{f}_0)(\underline{\varepsilon}(\mathbf{f}_0))^{\mathbf{H}} \qquad (2)$$

where $\alpha = \frac{1}{\mathbf{M}} \sum_{\mathbf{j}=1}^{\mathbf{M}} \int |\mathbf{s}_\mathbf{j}(\mathbf{t}, \mathbf{f}_0)|^2 \mathbf{dt}$.

If the assumption that a single phase is present is correct, the covariance matrix as shown in equation (2) is rank one and the steering vector may be obtained as the principal eigenvector of the matrix. This line of reasoning can be extended to calibrate the entire wavetrain for events from a particular region. However, the signal can no longer be considered to be stationary, even approximately. The signal model must be extended to permit changing spatial covariance structure along the wavetrain. We propose the following narrowband model:

$$\underline{\mathbf{r}}(\mathbf{t}) = \underline{\mathbf{E}}(\mathbf{f}_0)\underline{\mathbf{S}}(\mathbf{t}, \mathbf{f}_0)\mathbf{e}^{-\mathbf{i}2\pi\mathbf{f}_0\mathbf{t}} = \left[\underline{\varepsilon}_1\ \underline{\varepsilon}_2\ \cdots\ \underline{\varepsilon}_\mathbf{d}\right]\begin{bmatrix}\mathbf{s}^1(\mathbf{t})\\ \mathbf{s}^2(\mathbf{t})\\ \cdot\\ \cdot\\ \cdot\\ \mathbf{s}^\mathbf{d}(\mathbf{t})\end{bmatrix}\mathbf{e}^{-\mathbf{i}2\pi\mathbf{f}_0\mathbf{t}} \tag{3}$$

This is a collection of $\mathbf{d}$ signals representing all of the phases present, which may be a great number if multipath arrivals are considered. For simplicity, the frequency dependence of the model has been suppressed, but it is understood that the $\mathbf{d}$ individual steering vectors and baseband signals are functions of $\mathbf{f}_0$. The support of the individual baseband phase signals $\mathbf{s}^\mathbf{i}(\mathbf{t})$ may be expected to be transient. With phases coming and going, the spatial structure of the signals will vary as first one steering vector, then another comes to dominate array signal. At higher frequencies, as scattering becomes more significant, it is likely that multiple steering vectors will be required simultaneously to capture the range of spatial structure of signals originating from a specific source region.

$$\underline{\mathbf{R}}(\mathbf{t}_1, \mathbf{t}_2) = \overline{\underline{\mathbf{r}}(\mathbf{t}_1)(\underline{\mathbf{r}}(\mathbf{t}_2))^\mathbf{H}} \sim \left[\underline{\varepsilon}_1\ \underline{\varepsilon}_2\ \cdots\ \underline{\varepsilon}_\mathbf{d}\right]\left(\frac{1}{\mathbf{M}}\sum_{\mathbf{j}=1}^{\mathbf{M}}\begin{bmatrix}\mathbf{s}_\mathbf{j}^1(\mathbf{t}_1)\\ \mathbf{s}_\mathbf{j}^2(\mathbf{t}_1)\\ \cdot\\ \cdot\\ \cdot\\ \mathbf{s}_\mathbf{j}^\mathbf{d}(\mathbf{t}_1)\end{bmatrix}\begin{bmatrix}\mathbf{s}_\mathbf{j}^1(\mathbf{t}_2)\\ \mathbf{s}_\mathbf{j}^2(\mathbf{t}_2)\\ \cdot\\ \cdot\\ \cdot\\ \mathbf{s}_\mathbf{j}^\mathbf{d}(\mathbf{t}_2)\end{bmatrix}^\mathbf{H}\right)\left[\underline{\varepsilon}_1\ \underline{\varepsilon}_2\ \cdots\ \underline{\varepsilon}_\mathbf{d}\right]^\mathbf{H} \tag{4}$$

It is convenient to compute and represent samples of the covariance function of equation (4) in discrete form as a matrix

$$\underline{\mathbf{R}} = \begin{bmatrix}\underline{\mathbf{R}}(0,0) & \underline{\mathbf{R}}(0,\Delta\mathbf{t}) & \underline{\mathbf{R}}(0,2\Delta\mathbf{t}) & \cdots & \underline{\mathbf{R}}(0,\mathbf{P}\Delta\mathbf{t})\\ \underline{\mathbf{R}}(\Delta\mathbf{t},0) & \underline{\mathbf{R}}(\Delta\mathbf{t},\Delta\mathbf{t}) & \underline{\mathbf{R}}(\Delta\mathbf{t},2\Delta\mathbf{t}) & \cdots & \underline{\mathbf{R}}(\Delta\mathbf{t},\mathbf{P}\Delta\mathbf{t})\\ \underline{\mathbf{R}}(2\Delta\mathbf{t},0) & \underline{\mathbf{R}}(2\Delta\mathbf{t},\Delta\mathbf{t}) & \underline{\mathbf{R}}(2\Delta\mathbf{t},2\Delta\mathbf{t}) & \cdots & \underline{\mathbf{R}}(2\Delta\mathbf{t},\mathbf{P}\Delta\mathbf{t})\\ \cdots & \cdots & \cdots & \cdots & \cdots\\ \underline{\mathbf{R}}(\mathbf{P}\Delta\mathbf{t},0) & \underline{\mathbf{R}}(\mathbf{P}\Delta\mathbf{t},\Delta\mathbf{t}) & \underline{\mathbf{R}}(\mathbf{P}\Delta\mathbf{t},2\Delta\mathbf{t}) & \cdots & \underline{\mathbf{R}}(\mathbf{P}\Delta\mathbf{t},\mathbf{P}\Delta\mathbf{t})\end{bmatrix} \tag{5}$$

An example covariance matrix for the signals from the Kirovsk mine observed by four of the channels (ARA0, ARD1, ARD4, ARD7) of ARCES is shown in Figure 6. This covariance matrix was computed for a narrow band around 2.5 Hz using 236 events. The moduli of the individual (complex) elements of the matrix are represented in grayscale in the image with the darker elements having larger moduli. The individual phases (Pn, Pg, Sn and Lg) are apparent in the matrix. It is interesting to note that the separate phases are correlated. Some decorrelation might be expected given the relative moveout of the different phases as the events are distributed over some source region. In

this case, the source region is small (several kilometers in extent), which may account for the relatively high cross-correlations among the phases.

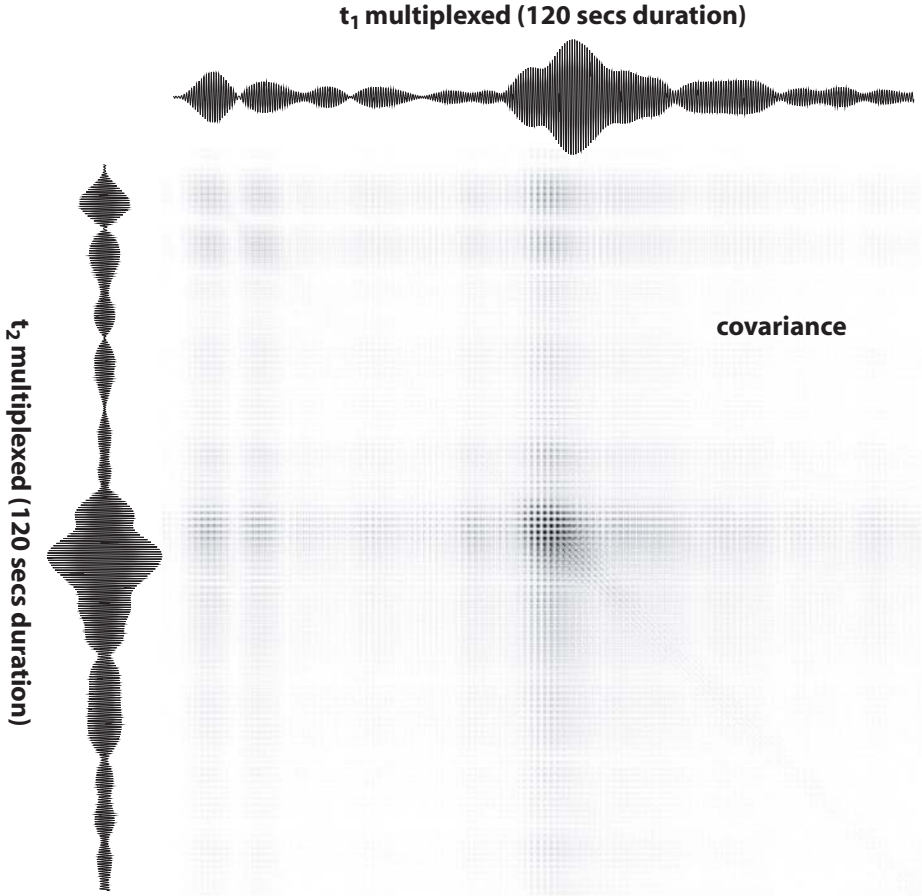

Figure 6. Example covariance matrix for 236 events from the Kirovsk mine on the Khibiny massif as recorded by a subset of the ARCES array. Note the correlations between the different phase types: Pn, Pg, Sn, and Lg.

It is our intention to extract systematically from covariance matrices of the type shown time-varying steering vectors for particular source regions and for a large number of narrow bands. We anticipate using these steering vectors in beamforming operations that use the entire time-history of the signal in an temporally incoherent, but spatially coherent detection operation.

CONCLUSIONS AND RECOMMENDATIONS

We have constructed a prototype algorithm for the fully-automatic identification and location of seismic events from a given source region. This has been applied to a wide range of sources of repeating seismicity in Fennoscandia and North West Russia, and in Kazakhstan. The use of carefully calibrated processing parameters has led to greatly increased stability in location estimates which in many situations are comparable to solutions obtained interactively by an analyst. We have also documented a situation whereby the fully automatic template-based location estimates were significantly better than those obtained by an analyst. This is due to the fact that the solutions obtained are heavily influenced by the backazimuth estimates obtained from a regional array station and these are estimates vary with the applied frequency band. For each phase analyzed, the analyst makes a decision of which frequency band to use and does not have available information regarding which frequency band is optimal for that particular site (we have also demonstrated that the optimal frequency band varies significantly from site to site). The template-based automatic system also applies a calibrated correction term to the backazimuth measurement prior to the location

procedure which takes into account the azimuth bias associated with the specific frequency band applied. An analyst would require detailed calibration information for the site involved in order to know how great a correction to apply for the processing parameters chosen. This scenario motivates a completely different approach whereby the steering vectors applied during F-K analysis are modified to take account of the demonstrable apparent curvature of the wavefield with frequency, in order to provide a slowness estimate with a zero bias for all frequency bands. It is not yet known to which degree such a calibration is possible. The greatest unknown is the extent to which the time-delay corrections are a continuous function of the theoretical slowness vector.

Towards the aim of source-region-specific detection procedures, in situations where complicated and highly heterogeneous source-time functions preclude the effective use of waveform correlation detectors, we anticipate that time-varying steering vectors calculated from multiple narrow-band observations of large numbers of events from that region will facilitate an effective beamforming operation which utilizes the full wavetrain.

ACKNOWLEDGEMENTS

We are grateful to Vladimir Asming and colleagues at the Kola Regional Seismological Center in Apatity, Russia, for collecting Ground Truth information from the Russian mine-operating companies as to the sites and times of routine industrial explosions. We would also like to thank staff at the Kazakhstan National Data Center for providing data from the Kazakhstan array network together with automatic and reviewed event bulletins.

REFERENCES

Gibbons, S. J., T. Kværna and F. Ringdal (2005), Monitoring of seismic events from a specific source region using a single regional array, in *J. Seismol.* 9: 277-294.

Gibbons, S. J. and Ringdal, F. (2006), The detection of low magnitude seismic events using array-based waveform correlation, in *Geophys. J. Int*. 165: 149-166.

Harris, D. B., F. Ringdal, E. O. Kremenetskaya, S. Mykkeltveit, J. Schweitzer, T. F. Hauk, V. E. Asming, D. W. Rock and J. P. Lewis (2003). Ground-truth collection for mining explosions in Northern Fennoscandia and Russia, in *Proceedings of the 25th Seismic Research Review - Nuclear Explosion Monitoring: Building the Knowledge Base*, LA-UR-03-6029, Vol. 1, pp. 54-63.

Kværna, T., S. J. Gibbons, F. Ringdal, and D. B. Harris (2004). Integrated seismic event detection and location by advanced array processing, in *Proceedings of the 26th Seismic Research Review - Trends in Nuclear Explosion Monitoring*, LA-UR-04-5801, Vol. 2, pp. 742-751.

Kværna, T., S. J. Gibbons, F. Ringdal, and D. B. Harris (2005). Integrated Seismic Event Detection and Location by Advanced Array Processing, in *Proceedings of the 27th Seismic Research Review - Ground-based Nuclear Explosion Monitoring Techniques*, LA-UR-05-6407, Vol. 2, pp. 927-937.

Kværna, T. and F. Ringdal (1989), A multichannel processing approach to real time network detection, phase association and threshold monitoring, in *Bull. Seism. Soc. Am.* 79: 1927-1940.